STATIC BENDING ANALYSIS OF FGP L-SHAPE NANOPLATES RESTING ON ELASTIC FOUNDATION USING FEM BASED ON NONLOCAL THEORY

TRAN THE VAN[1], PHAM QUOC HOA[1*], LE THANH DANH[1], AO HUNG LINH[1],
TRAN TRUNG THANH [2]
[1] *Faculty of Mechanical Technology, Industrial University of Ho Chi Minh City*
[2] *Faculty of Mechanical Engineering, Le Quy Don Technical University*
Corresponding author: phamquochoa@iuh.edu.vn
DOIS: https://doi.org/10.46242/jstiuh.v60i06.4628

Abstract. This article presents a finite element method for static bending analysis of the functionally graded porous (FGP) L-shape nanoplate resting on the elastic foundation (EF) using the nonlocal elasticity theory. The FGP materials with two-parameter are the volume fraction index (k) and the porosity volume fraction (ξ) in two cases of even and uneven porosity. The EF includes Winkler-stiffness (k_1) and Pasternak-stiffness (k_2). Some numerical results of the proposed method are compared with those of published works to verify accuracy and reliability. Furthermore, the effects of some elastic foundation factors and material properties of static bending of FGP nanoplates resting on the EF are studied in detail.
Keywords. FGP; bending; nanoplates; nonlocal elasticity theory.

1 INTRODUCTION

Nowadays, with the sophisticated development of science and technology, the investigation of nanostructures has been deeply concerned by scientists in the world. They are applied to many fields such as bio-engineering, nano-electromechanical devices and actuators, etc due to their exceptional mechanical, thermal, and electrical properties.

In order to calculate for nano-structures, many theories have been proposed such as the modified couple stress theory [1], the strain gradient theory [2], and the nonlocal theory [3], [4]. Among these theories, the nonlocal theory is used popularly in the literature for simplicity and accuracy. For example, Li et al. [5] developed a new nonlocal model to solve the static and dynamic problems for circular elastic nano-solids. Ansari et al. [6], [7] used nonlocal theory to consider the free vibration of a single-layered graphene plate. In [7], Arash and co-workers commented about nonlocal theory in modelling carbon nanotubes and graphene. Farajpouret al. [8] studied thermomechanical vibration of graphene plates including surface effects by decoupling the nonlocal elasticity equations. Jalali et al. [9] used molecular dynamics combining with nonlocal elasticity approaches to investigate the effect of out-of-plane defects on vibration analysis of graphene. In addition, the nonlocal theory employed to investigate the various performances of nanoplates is also shown in [10].

With analysis of nanostructures resting on EF, some typical work as Wang and Li [11] computed the static bending of the nanoplates resting on the EF. Narendar and Gopalakrishnan et al. [12] studied the wave dispersion of a single-layered graphene sheet embedded in an elastic polymer matrix. Pouresmaeeli et al. [13] investigated the vibration behaviors of nanoplates placed on a viscoelastic medium. Sobhy [14] used an analytical method (AM) based on nonlocal theory to examine static bending, free vibration, mechanical buckling, and thermal buckling of functionally graded material (FGM) nanoplates lying on the EF.

The FGP material is a form of FG material with the appearance of internal porosity. Most studies are shown that the increase of the porosity leads to reduce the stiffness of structures. However, with outstanding features such as lightweight, excellent energy-absorbing capability, great thermal resistant properties, etc., they have been widely applied in many fields including aerospace, automotive industry, and civil engineering. Some typical works studying FGP structure can be found in the literature [15]-[19]. Recently, FGP materials have been also used for nanostructures, numerical results on mechanical behavior analysis of nanostructures are provided in documents [20]-[24]. In these studies, they mainly use analytical methods

and thus are limited in complex problem models and different boundary conditions. So it motivated us to develop an efficient numerical method to fill this gap.

From the analysis of the above literature, according to the best of the authors' knowledge, the static bending analysis of FGP L-shape nanoplates resting on EF has been not published yet. In this work, we use the eight-node quadrilateral (Q8) element combining with the nonlocal theory to accurately describe the stress-strain and displacement field of the FGP L-shape nanoplate resting on the EF. The accuracy and reliability of the current method are verified by performing an example to compare the obtained results with those available in the previously published literature. Moreover, the effects of geometry parameters and material properties on the static bending of FGP nanoplates are examined in detail.

2 GOVERNING EQUATIONS

2.1 The FGP L-shape nanoplates

As it is known, L-shape structures with the advantage of saving space, flexibly arranging components in a small space. They are being applied in electronic devices such as CPUs, GPUs, etc. In this study, we consider FGP L-shape nanoplates with geometrical parameters as shown in Fig. 1.

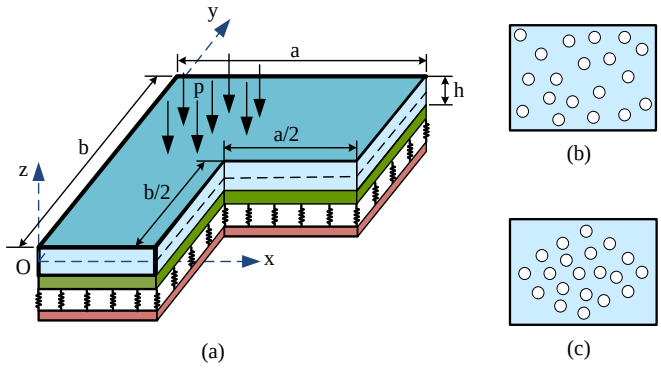

Fig. 1. The FGP L-shape nanoplate resting on the EF.
(a) L-shaped nano-plate, (b) Even porosity, (c) Uneven porosity

The FGP materials with the variation of two constituents and two different distributions of porosity through-thickness are presented as [25]:

$$\text{Case 1: } P(\text{z}) = P_m + (P_c - P_m)\left(\frac{z}{h} + 0{,}5\right)^k - \frac{\xi}{2}(P_c + P_m) \tag{1}$$

$$\text{Case 2: } P(\text{z}) = P_m + (P_c - P_m)\left(\frac{z}{h} + 0{,}5\right)^k - \frac{\xi}{2}(P_c + P_m)\left(1 - \frac{2|z|}{h}\right) \tag{2}$$

with P represents the effective material properties such as Young's modulus E, mass density ρ and Poisson's ratio υ. the Case 1, case 2 are respectively the modified mixture rule for the two components with even porosity and uneven porosity. Symbols "m" and "c" denote the typical material properties at the bottom (metal) and top surfaces (ceramic) of the nanoplate, respectively; k is the volume fraction index while ξ ($\xi \le 1$) represents the porosity volume fraction.

2.2 Nonlocal elasticity theory

According to the nonlocal theory, the stress-strain relation is determined by [4]:

$$\left(1 - \mu\nabla^2\right)\boldsymbol{\sigma} = \mathbf{Q} \tag{3}$$

in which: $\mu = (e_0 l)^2$ is a nonlocal factor ($0 \le \mu \le 4$), l is an internal characteristic length and e_0 is a constant, $\mathbf{Q}$ is the stress tensor at a point which is calculated follows the local theory, $\nabla^2 = \frac{\partial^2}{\partial x^2} + \frac{\partial^2}{\partial y^2}$ is the Laplacian operator and thus the small-scale effect depends on the atomic and/or molecular mechanical/electrical/chemical characteristics are taken into account. Note that, when $l = 0$ ($\mu = 0$), the nonlocal theory will become the classical plate theory.

2.3 The displacement fields

Based on the first-order shear deformation theory (FSDT), the displacement field of the FGP nanoplate is given by:

$$\begin{cases} u(x,y,z) = u_0(x,y) + z\theta_y(x,y); \\ v(x,y,z) = v_0(x,y) + z\theta_x(x,y); \\ w(x,y,z) = w_0(x,y). \end{cases} \tag{4}$$

with u_0, v_0, w_0 are the displacement components at the mid-plane (z = 0) along x, *y*, *z*-axis; θ_x, θ_y are the angle of rotation of the middle surface via the *y* and *x*-axis, respectively.

2.4 The strain vectors

The strain vector of the plate is defined by [12]:

$$\boldsymbol{\varepsilon} = \begin{Bmatrix} \varepsilon_{xx} \\ \varepsilon_{yy} \\ \varepsilon_{xy} \\ \varepsilon_{xz} \\ \varepsilon_{yz} \end{Bmatrix} = \begin{Bmatrix} u_{,x} \\ v_{,y} \\ u_{,y} + v_{,x} \\ w_{,x} + u_{,z} \\ w_{,y} + v_{,z} \end{Bmatrix} = \begin{Bmatrix} u_{0,x} \\ v_{0,y} \\ u_{0,y} + v_{0,x} \\ v_{0.x} + \theta_x \\ w_{0,y} + \theta_y \end{Bmatrix} + z \begin{Bmatrix} \theta_{\mathrm{x},x} \\ \theta_{\mathrm{y},y} \\ \theta_{x,y} + \theta_{\mathrm{y},x} \\ 0 \\ 0 \end{Bmatrix} \tag{5}$$

Rewritten in shortened form as follows:

$$\boldsymbol{\varepsilon} = \begin{Bmatrix} \boldsymbol{\varepsilon}_1 \\ \boldsymbol{\varepsilon}_2 \end{Bmatrix} = \begin{Bmatrix} \boldsymbol{\varepsilon}_1^0 + z\boldsymbol{\varepsilon}_1^1 \\ \boldsymbol{\varepsilon}_2^0 \end{Bmatrix} \tag{6a}$$

in which

$$\boldsymbol{\varepsilon}_1 = \begin{Bmatrix} \varepsilon_{xx} \\ \varepsilon_{yy} \\ \varepsilon_{xy} \end{Bmatrix}; \boldsymbol{\varepsilon}_2 = \begin{Bmatrix} \varepsilon_{xz} \\ \varepsilon_{yz} \end{Bmatrix}; \boldsymbol{\varepsilon}_1^0 = \begin{Bmatrix} u_{0,x} \\ v_{0,y} \\ u_{0,y} + v_{0,x} \end{Bmatrix}; \boldsymbol{\varepsilon}_1^1 = \begin{Bmatrix} \theta_{x,x} \\ \theta_{y,y} \\ \theta_{x,\mathrm{y}} + \theta_{\mathrm{y},x} \end{Bmatrix}; \boldsymbol{\varepsilon}_2^0 = \begin{Bmatrix} w_{0,x} + \theta_x \\ w_{0,y} + \theta_y \end{Bmatrix} \tag{6b}$$

2.5 The stress-strain relation

Following Hooke's law, the stress tensor at any point of nanoplates is determined by:

$$\mathbf{Q} = \mathbf{D}.\boldsymbol{\varepsilon} \tag{7}$$

$$\mathbf{D} = \begin{bmatrix} \mathbf{D}_\mathrm{b} & \mathbf{0}_{3\times 2} \\ \mathbf{0}_{2\times 3} & \mathbf{D}_\mathrm{s} \end{bmatrix}; \mathbf{D}_\mathrm{b} = \begin{bmatrix} C_{11} & C_{12} & 0 \\ & C_{22} & 0 \\ sym & & C_{66} \end{bmatrix}; \mathbf{D}_\mathrm{s} = \begin{bmatrix} C_{55} & 0 \\ 0 & C_{44} \end{bmatrix} \tag{8}$$

$$C_{11} = C_{22} = \frac{E}{(1-\nu^2)}; C_{12} = \frac{\nu E}{(1-\nu^2)}; C_{66} = C_{55} = C_{44} = \frac{E}{2(1+\nu)} \tag{9}$$

The equation represents the relationship between the internal forces and the deformation components are written in the form:

$$\left\{N_{xx} \quad N_{yy} \quad N_{xy}\right\} = \mathbf{A}\boldsymbol{\varepsilon}_1^0 + \mathbf{B}\boldsymbol{\varepsilon}_1^1; \left\{M_{xx} \quad M_{yy} \quad M_{xy}\right\} = \mathbf{B}\boldsymbol{\varepsilon}_1^0 + \mathbf{H}\boldsymbol{\varepsilon}_1^1; \left\{Q_{xz} \quad Q_{yz}\right\} = \mathbf{A}^s\boldsymbol{\varepsilon}_2^0 \tag{10}$$

where $\mathbf{A}; \mathbf{B}; \mathbf{H}; \mathbf{A}^s$ are determined as follows

$$\left(\mathbf{A}; \mathbf{B}; \mathbf{H}\right) = \int_{-h/2}^{h/2} \mathbf{D}_b.(1; z; z^2)\,\mathrm{d}z\,; \;\; \mathbf{A}^s = \frac{5}{6}\int_{-h/2}^{h/2} \mathbf{D}_s.\mathrm{d}z \tag{11}$$

2.6 The plate element

We use the eight-node plate element each node has five degrees of freedom (DOF). The nodal displacement vector can be defined as follows:

$$\mathbf{d}_e = [\mathbf{d}_1^T \quad \mathbf{d}_2^T \quad \mathbf{d}_3^T \quad \mathbf{d}_4^T \quad \mathbf{d}_5^T \quad \mathbf{d}_6^T \quad \mathbf{d}_7^T \quad \mathbf{d}_8^T]^T \tag{12}$$

The displacements at the node $i\ (i = 1 \div 8)$ of the element are expressed as

$$\mathbf{d}_i = \left\{u_{0i} \quad v_{0i} \quad w_{0i} \quad \varphi_{xi} \quad \varphi_{yi}\right\} \tag{13}$$

The displacements field in the plate element is interpolated through the displacement node as

$$u_0 = \mathbf{N}_u.\mathbf{d}_e; \; v_0 = \mathbf{N}_v.\mathbf{d}_e; \; w_0 = \mathbf{N}_w.\mathbf{d}_e; \; \varphi_x = \mathbf{N}_{\varphi x}.\mathbf{d}_e; \; \varphi_y = \mathbf{N}_{\varphi y}.\mathbf{d}_e \tag{14}$$

where $\mathbf{N}_u, \mathbf{N}_v, \mathbf{N}_w, \mathbf{N}_{\varphi x}, \mathbf{N}_{\varphi y}$ are the shape functions:

$$\begin{cases} \mathbf{N}_u = \left[\mathbf{N}_1^{(1)} \quad \mathbf{N}_2^{(1)} \quad \ldots \quad \mathbf{N}_7^{(1)} \quad \mathbf{N}_8^{(1)}\right]; \mathbf{N}_v = \left[\mathbf{N}_1^{(2)} \quad \mathbf{N}_2^{(2)} \quad \ldots \quad \mathbf{N}_7^{(2)} \quad \mathbf{N}_8^{(2)}\right]; \\ \mathbf{N}_w = \left[\mathbf{N}_1^{(3)} \quad \mathbf{N}_2^{(3)} \quad \ldots \quad \mathbf{N}_7^{(3)} \quad \mathbf{N}_8^{(3)}\right]; \mathbf{N}_{\varphi x} = \left[\mathbf{N}_1^{(4)} \quad \mathbf{N}_2^{(4)} \quad \ldots \quad \mathbf{N}_7^{(4)} \quad \mathbf{N}_8^{(4)}\right]; \\ \mathbf{N}_{\varphi y} = \left[\mathbf{N}_1^{(5)} \quad \mathbf{N}_2^{(5)} \quad \ldots \quad \mathbf{N}_7^{(5)} \quad \mathbf{N}_8^{(5)}\right]. \end{cases} \tag{15}$$

The matrices $N_i^{(j)}\ \left(j = 1 \div 5\right)$ are given by

$$\begin{cases} \mathbf{N}_i^{(1)} = \left[\psi_i \quad 0 \quad 0 \quad 0 \quad 0\right]; \mathbf{N}_i^{(2)} = \left[0 \quad \psi_i \quad 0 \quad 0 \quad 0\right]; \\ \mathbf{N}_i^{(3)} = \left[0 \quad 0 \quad \psi_i \quad 0 \quad 0\right]; \mathbf{N}_i^{(4)} = \left[0 \quad 0 \quad 0 \quad \psi_i \quad 0\right]; \\ \mathbf{N}_i^{(5)} = \left[0 \quad 0 \quad 0 \quad 0 \quad \psi_i\right]. \end{cases} \tag{16}$$

where $\psi_i\ \psi_i$ is the Lagrange interpolation function.

The element stiffness matrix is determined by

$$\mathbf{K}_e = \mathbf{K}_e^p + \mathbf{K}_e^f \tag{17}$$

with $\mathbf{K}_e^p, \mathbf{K}_e^f$ are the element plate stiffness matrix, and the element foundation stiffness matrix, respectively.

in which

$$\mathbf{K}_e^b = \int_{S_e} \left(\begin{bmatrix} \mathbf{B}_1 & \mathbf{B}_2 \end{bmatrix}^T \begin{bmatrix} \mathbf{A} & \mathbf{B} \\ \mathbf{B} & \mathbf{H} \end{bmatrix} \begin{bmatrix} \mathbf{B}_1 \\ \mathbf{B}_2 \end{bmatrix} + \left(\mathbf{B}_3^T \mathbf{A}^s \mathbf{B}_3\right) \right) dxdy \tag{18}$$

$$\begin{aligned} \mathbf{K}_e^f = \int_{S_e} & k_1 \left(\mathbf{N}_w^T \mathbf{N}_w + \mu\left(\mathbf{N}_{w,x}^T \mathbf{N}_{w,x} + \mathbf{N}_{w,y}^T \mathbf{N}_{w,y}\right)\right) + k_2 (\mathbf{N}_{w,x}^T \mathbf{N}_{w,x} + \mathbf{N}_{w,y}^T \mathbf{N}_{w,y} \\ & + \mu(\mathbf{N}_{w,xx}^T \mathbf{N}_{w,xx} + \mathbf{N}_{w,yy}^T \mathbf{N}_{w,yy} + \mathbf{N}_{w,xx}^T \mathbf{N}_{w,yy} + \mathbf{N}_{w,yy}^T \mathbf{N}_{w,xx})) dxdy \end{aligned} \tag{19}$$

where

$$\mathbf{B}_1 = \begin{bmatrix} \mathbf{N}_{u,x} \\ \mathbf{N}_{v,y} \\ \mathbf{N}_{u,x} + \mathbf{N}_{v,y} \end{bmatrix}; \mathbf{B}_2 = \begin{bmatrix} \mathbf{N}_{\varphi x,x} \\ \mathbf{N}_{\varphi y,y} \\ \mathbf{N}_{\varphi x,y} + \mathbf{N}_{\varphi y,x} \end{bmatrix}; \mathbf{B}_3 = \begin{bmatrix} \mathbf{N}_{w,x} + \mathbf{N}_{\varphi x} \\ \mathbf{N}_{w,y} + \mathbf{N}_{\varphi y} \end{bmatrix} \tag{20}$$

$$\mathbf{N} = \left[\mathbf{N}_u^T \quad \mathbf{N}_v^T \quad \mathbf{N}_w^T \quad \mathbf{N}_{\varphi x}^T \quad \mathbf{N}_{\varphi y}^T\right] \tag{21}$$

The element force vector is given as follows: $\mathbf{F}_{\mathrm{e}} = \int_S p\left(1-\mu\nabla^2\right)\mathbf{N}_w^T dS$ (22)

where

$$\mathbf{N}_w = [0\,0\,N_1\;0\,0,...,0\,0\,N_8\;0\,0] \tag{23}$$

For the static problem:

$$\mathbf{K.q} = \mathbf{F} \tag{24}$$

in which **K**, **F**, **q** are the global stiffness matrix, the global force vector, and the global displacement vector. They are gathered from the element stiffness matrix, the element force vector, and the element displacement vector.

3 VERIFICATION PROBLEM

In this section, based on the finite element formula established in section 3, the authors code a calculation program in Matlab software. Then, an example is performed to verify the reliability of the calculation program.

For that purpose, we consider fully simply supported (FSS) FGM nanoplates with geometry parameters: $a=b=10$ *nm*, $h=a/10$; and material properties: metal (Al) $E_1=70$ *GPa*; ceramic (Al_2O_3) $E_2=380$ *GPa*, and $\upsilon=0.3$ is fixed. Herein, dimensionless quantities are introduced by

$$w^* = \frac{100E_2h^3}{q_0a^4}w,\ \sigma_{xx}^* = \frac{10h}{q_0a}\sigma_{xx},\ \sigma_{xy}^* = \frac{10h}{q_0a}\sigma_{xy},\ K_1 = \frac{k_1a^4}{H},\ K_2 = \frac{k_2a^2}{H},\ H = \frac{E_2h^3}{12(1-\nu^2)} \tag{25}$$

Table 1. The displacement and stress of FGM nanoplates resting on the EF (k=0, K_2=0).

Method	K_1	$\mu=0$		$\mu=4$	
		w^*	σ_{xx}^*	w^*	σ_{xx}^*
[14]	0	2.9603	19.9550	5.2977	35.7108
	100	2.3290	15.6991	3.5671	24.0455
Present	0	2.9600	19.8990	5.2971	35.6106
	100	2.3288	15.6555	3.5669	23.9791

As exhibited in Table 1, the present results are very in agreement with those of Sobhy [14] using Navier's solution. Note that, Navier's solution can only be applied to nanoplates with simply supported boundary conditions. From the above example, it is possible to confirm the accuracy and reliability of the calculation program.

4 NUMERICAL RESULTS

Firstly, the FGP L-shape nanoplates (as Fig. 1) with geometry parameters and material properties as in section 3. The FGP L-shape nanoplate is subjected to uniformly load p_0 in perpendicular directions. The deformation field of the FSS FGP L-shape nanoplate is indicated in Fig. 2a. The stresses of A-point with coordinates (5, 5.625) through the thickness of the FGP L-shape nanoplate is presented in Fig. 2c, 2d. There is a difference in the stress distribution at a point along the thickness of the nanoplate in two cases because the stiffness of the nanoplate changes in each case according to different laws depending on the variable z.

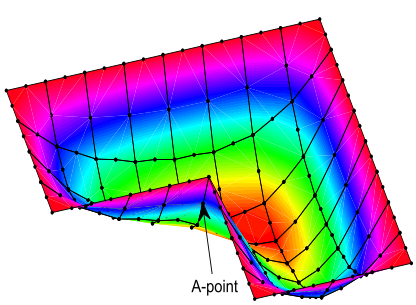

a) The deformation field

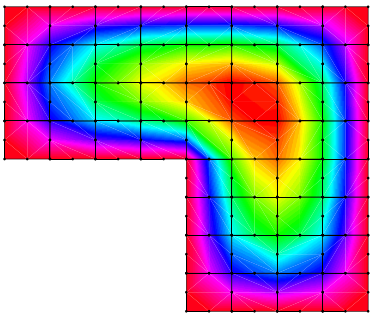

b) The top view deformation field

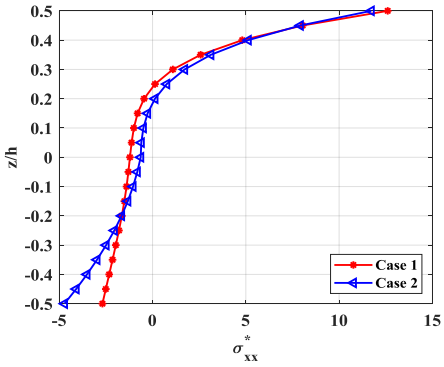

c) The stress σ^*_{xx} at A-point

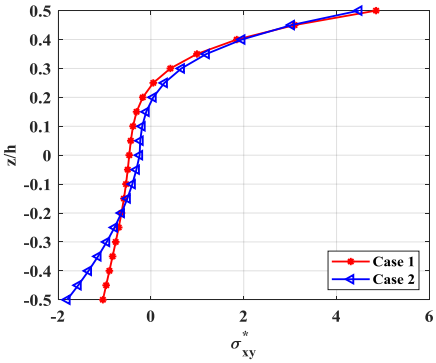

d) The stress σ^*_{xy} at A-point

Fig. 2. The deformation and stresses of the FSS FGP L-shape nanoplate (k=5, $\xi = 0.2$, $\mu = 4$, K_1=100, K_2=10).

4.1 Effect of the volume fraction index k

Secondly, the volume fraction index *k* gets values from 0 to 100. The FSS FGP L-shape nanoplate with porosity volume fraction $\xi = 0.2$, nonlocal factor $\mu = 4$. The stiffness of foundation: K_1=100, K_2=10. From Fig. 3, it can be seen that when *k* increases lead to the displacement of nanoplates increase due to the stiffness of nanoplates decrease. We also find that the displacement of the FGP L-shape nanoplate decreases rapidly when *k* is in the range 0-20 and the displacement of the nanoplate with porosity distribution in case 2 is smaller than those of case 1 because the stiffness of the case 2 is larger than the stiffness of case 1. This can be easily obtained when comparing Eq. (1) and Eq. (2).

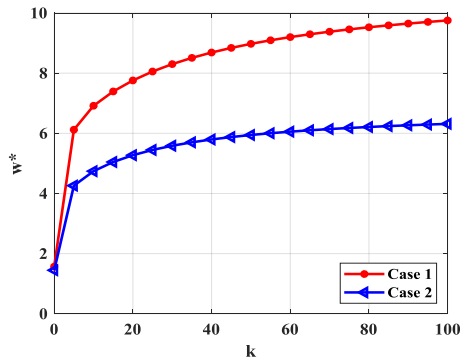

Fig. 3. The maximum displacement of the FSS FGP L-shape nanoplate versus volume fraction index *k*.

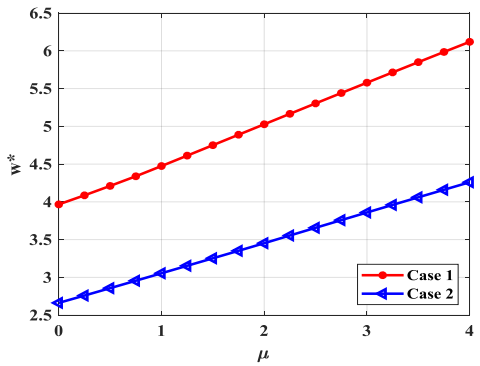

Fig. 4. The maximum displacement of the FSS FGP L-shape nanoplate versus nonlocal factor μ.

4.2 Effect of the nonlocal factor μ

Next, the authors choose the nonlocal factor in range $\mu = 0 \div 4$ with $\mu = 0$ is the classical plate. The FSS FGP

L-shape nanoplate with porosity volume fraction $\xi = 0.2$, volume fraction index k=5. The stiffness of foundation: K_1=100, K_2=10. It can be found that when the nonlocal factor μ increases lead to displacement increase due to the nonlocal factor makes reduce the stiffness of the FGP L-shape nanoplate (see Fig. 4).

4.3 Effect of the stiffness of foundation

Finally, in order to consider the influences of the stiffness of foundation on the static bending of the FFSS FGP L-shape nanoplate, we change K_1 from 0 to 1000, and K_2 from 0 to 100 with respect to k=5, ξ=0.2, and nonlocal factor μ=4. From the obtained numerical results show in Fig. 5, it is observed that when increasing K_1 and K_2 leads to the displacement of nanoplates decrease and thus, the elastic foundation makes the stiffness of FGP L-shape nanoplates increase. Furthermore, it is found that the Pasternak foundation supports stronger than the Winkler foundation.

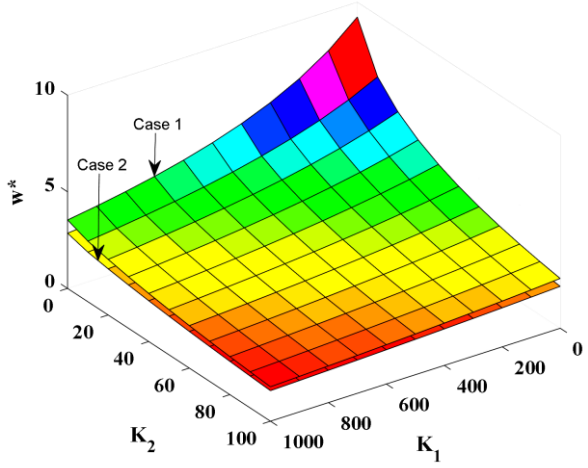

Fig. 5. The displacement of the FSS FGP L-shape nanoplate versus K_1 and K_2.

5 CONCLUSIONS

In this article, the static analysis of the FGP L-shape nanoplate is studied by using the FEM and nonlocal theory. From the finite element formulation, the author coded the calculation program by Matlab software. Checking the reliability of the calculation program and performing the examples to analyze the effect of parameters on static bending of FGP L-shape nanoplates. From the proposed formulation and the numerical results, some main remarks are drawn as follows:

- Using the FEM will be convenient in modelling and meshing. Especially, with structures that are not symmetrical as L-shape.

- The material parameters and the law of porosity distribution significantly affect the static bending of FGP L-shape nanoplates. Specifically, the increase of volume fraction index k and porosity volume fraction ξ make the reduction of the stiffness of nanoplates and this leads to the increase of displacement and stress. Conversely, the increase of foundation's stiffness results in decrease displacement and stress of nanoplates. In addition, it can be seen that the nanoplates with porosity distribution case 2 is stiffer than case 1.

- Numerical results in the present work are useful for the calculation, design of FGP L-shape nanoplates in engineering and technologies.

- The present approach can be developed to investigate static bending of the FGP nanoplate with different shapes.

REFERENCES

[1]. Yang F, Chong ACM, Lam DCC, Tong P. Couple stress-based strain gradient theory for elasticity. *Int J Solids Struct*, 39: 2731-43, 2002.

[2]. Aifantis EC. Strain gradient interpretation of size effects. *Int J Fract*, 95:1-4, 1999.

[3]. A. C. Eringen, "On differential equations of nonlocal elasticity and solutions of screw dislocation and surface waves", *Journal of Applied Physics*, vol. 54, no. 9, pp. 4703-4710, 1983.

[4]. A.C. Eringen, *Nonlocal Continuum Field Theories*, Springer: New York (NY), 2002.
[5]. C. Li, C.W. Lim, J. Yu, "Twisting statics and dynamics for circular elastic nanosolids by nonlocal elasticity theory", *Acta Mechanica Solida Sinica*, vol. 24, no. 6, pp. 484-94, 2011.
[6]. R. Ansari, S. Sahmani, B. Arash, "Nonlocal plate model for free vibrations of single-layered graphene sheets", *Physis Letter A*, vol. 375, no. 1, pp. 53-62, 2010.
[7]. B. Arash, Q. Wang, "A review on the application of nonlocal elastic models in modelling of carbon nanotubes and graphenes", *Computational Materials Science*, vol. 51, no. 1, pp. 303-313. 2012.
[8]. S. R. Asemi, A. Farajpour, Decoupling the nonlocal elasticity equations for thermomechanical vibration of circular graphene sheets including surface effects, *Physica E*, vol. 60, pp. 80-90. 2010.
[9]. S. K. Jalali, E. Jomehzadeh, N. M. Pugno, Influence of out-of-plane defects on vibration analysis of graphene: Molecular Dynamics and Nonlocal Elasticity approaches, *Superlattices and Microstructures*, vol. 91, pp. 331-344, 2016.
[10]. R. Ahababaei, J. N. Reddy, Nonlocal third-order shear deformation plate theory with application to bending and vibration of plate, *Journal of Sound and Vibration*, vol. 326, no 1-2, pp. 277-289, 2009.
[11]. Y. Z. Wang, F.M.Li, Static bending behaviors of nano-plate embedded in elastic matrix with small scale effects, *Mechanics Research Communications*, vol. 41, pp. 44-48, 2012.
[12]. S. Narendar, S. Gopalakrishnan S, Nonlocal continuum mechanics based ultrasonic flexural wave dispersion characteristics of a monolayer graphene embedded in polymer matrix, *Composites Part B: Engineering*, vol. 43, no. 8, pp. 3096-3103, 2012.
[13]. S. Pouresmaeeli, E. Ghavanloo, S. A. Fazelzadeh, Vibration analysis of viscoelastic orthotropic nano-plates resting on viscoelastic medium, *Composite Structures*, vol. 96, pp. 405-410, 2013.
[14]. Mohammed Sobhy, A comprehensive study on FGM nanoplates embedded in an elastic medium, *Composite Structures*, vol. 134, pp. 966-980, 2015.
[15]. G. Bansal, A. Gupta, V. Katiyar, Vibration of porous functionally graded plates with geometric discontinuities and partial supports, *Proceedings of the Institution of Mechanical Engineers, Part C: Journal of Mechanical Engineering Science* 234(21) (2020) 4149-4170.
[16]. A. Zenkour, Quasi-3D refined theory for functionally graded porous plates: displacements and stresses, *Physical Mesomechanics* 23(1) (2020) 39-53.
[17]. M.R. Barati, A.M. Zenkour, Electro-thermoelastic vibration of plates made of porous functionally graded piezoelectric materials under various boundary conditions, *Journal of Vibration and Control* 24(10) (2018) 1910-1926.
[18]. M.R. Barati, A.M. Zenkour, Analysis of postbuckling of graded porous GPL-reinforced beams with geometrical imperfection, *Mechanics of Advanced Materials and Structures* 26(6) (2019) 503-511.
[19]. A.A. Daikh, A.M. Zenkour, Effect of porosity on the bending analysis of various functionally graded sandwich plates, *Materials Research Express* 6(6) (2019) 065703.
[20]. Q.-H. Pham, T.T. Tran, V.K. Tran, P.-C. Nguyen, T. Nguyen-Thoi, A.M. Zenkour, Bending and hygro-thermo-mechanical vibration analysis of a functionally graded porous sandwich nanoshell resting on elastic foundation, *Mechanics of Advanced Materials and Structures* (2021) 1-21.
[21]. Q.-H. Pham, T.T. Tran, V.K. Tran, P.-C. Nguyen, T. Nguyen-Thoi, Free vibration of functionally graded porous non-uniform thickness annular-nanoplates resting on elastic foundation using ES-MITC3 element, *Alexandria Engineering Journal* (2021).
[22]. T.T. Tran, V.K. Tran, Q.-H. Pham, A.M. Zenkour, Extended four-unknown higher-order shear deformation nonlocal theory for bending, buckling and free vibration of functionally graded porous nanoshell resting on elastic foundation, *Composite Structures* 264 (2021) 113737.
[23]. M.H. Jalaei, H.-T. Thai, Dynamic stability of viscoelastic porous FG nanoplate under longitudinal magnetic field via a nonlocal strain gradient quasi-3D theory, *Composites Part B: Engineering* 175 (2019) 107164.
[24]. M.A. Abdulrazzaq, A.K. Muhammad, Z.D. Kadhim, N.M. Faleh, Vibration analysis of nonlocal strain gradient porous FG composite plates coupled by visco-elastic foundation based on DQM, *Coupled systems mechanics* 9(3) (2020) 201-217.
[25]. Shahsavari, D., M. Shahsavari, L. Li, and B. Karami, A novel quasi-3D hyperbolic theory for free vibration of FG plates with porosities resting on Winkler/Pasternak/Kerr foundation, *Aerospace Science and Technology*, 72, 2018, 134-149.

PHÂN TÍCH UỐN TĨNH CỦA TẤM NANO CHỮ L ĐẶT TRÊN NỀN ĐÀN HỒI SỬ DỤNG PHƯƠNG PHÁP PHẦN TỬ HỮU HẠN DỰA TRÊN LÝ THUYẾT PHI ĐỊA PHƯƠNG

TRẦN THẾ VĂN[1], PHẠM QUỐC HÒA[1], LÊ THANH DANH[1], AO HÙNG LINH[1], TRẦN TRUNG THÀNH[2]

[1]Khoa Cơ khí, Trường Đại học Công Nghiệp Thành phố Hồ Chí Minh

[2]Khoa Cơ khí-Học viện Kỹ thuật quân sự

Tóm tắt. Bài báo này trình bày phương pháp phần tử hữu hạn phân tích uốn tĩnh của tấm nano hình dạng L vật liệu xốp có cơ tính biến thiên đặt trên nền đàn hồi sử dụng lý thuyết phi địa phương (nonlocal). Vật liệu xốp có cơ tính biến thiên theo chỉ số mũ thể tích (k) và chỉ số lỗ rỗng (ξ) trong hai trường hợp phân bố lỗ rỗng "even" và "uneven". Nền đàn hồi bao gồm hai thông số là độ cứng Winkler (k_1) và độ cứng Pasternak (k_2). Một vài kết quả số được so sánh với kết quả của các công trình khác đã công bố để chứng minh tính chính xác và tin cậy của phương pháp đề xuất. Ngoài ra, ảnh hưởng của các tham số như độ cứng nền đàn hồi, đặc trưng vật liệu đến ứng xử uốn tĩnh của tấm nano đặt trên nền đàn hồi được nghiên cứu chi tiết trong phần kết quả số.

Từ khóa. FGP; Uốn tĩnh; Tấm nano; Lý thuyết phi địa phương.

Received on: 27/07/2021

Accepted on: 27/10/2021